DALTON
FULL PAPER

Complexation of uranium(VI) with acetate at variable temperatures

Jun Jiang,[a] Linfeng Rao,*[a] Plinio Di Bernardo,[b] PierLuigi Zanonato[b] and Arturo Bismondo[c]

[a] *Glenn T. Seaborg Center, Lawrence Berkeley National Laboratory, Berkeley, CA 94720, USA. E-mail: LRao@lbl.gov*
[b] *Università di Padova, via Loredan 4, Padova, 35131, Italy*
[c] *Istituto di Chimica e Tecnologie dei Materiali Avanzati del C.N.R. of Padova, Italy*

Received 25th July 2001, Accepted 31st January 2002
First published as an Advance Article on the web 14th March 2002

The complexation between uranium(VI) and acetate in 1.05 mol kg^{-1} $NaClO_4$ was studied at variable temperatures (25, 35, 45, 55 and 70 °C). The formation constants of three successive complexes, $UO_2(OOCCH_3)^+$, $UO_2(OOCCH_3)_2$ and $UO_2(OOCCH_3)_3^-$, and the molar enthalpies of complexation were determined by potentiometry and calorimetry. Extended X-ray Absorption Fine Structure Spectroscopy (EXAFS) provided structural information to identify the coordination modes of the acetate in the complexes in solution, which helped to interpret the trends in the enthalpy and entropy of the complexation. The effect of temperature on the stability of the complexes is discussed in terms of the electrostatic model.

1 Introduction

Recent activities in the environmental management of nuclear wastes have stimulated significant interest in the study of the coordination chemistry of actinides in solution, especially at elevated temperatures. For example, safe management and disposal of nuclear wastes require a better understanding of the complexation of actinides with organic and inorganic ligands at elevated temperatures, because the temperature in the nuclear waste storage tanks and the waste forms in the repository are significantly higher than the ambient temperature due to the radioactive decay energy.[1,2] Unfortunately, the majority of the thermodynamic data in the literature on the complexation of actinides are for 25 °C.[3] Extrapolation of these data to elevated temperatures by use of the van't Hoff isochore[4] may result in large errors if the enthalpy of complexation is temperature dependent and/or the temperature range of interest is wide.[5] More recent theoretical models developed by Helgeson and co-workers have considerably improved the accuracy in predicting the thermodynamic properties of aqueous species at high temperatures.[6–8] However, the application of these models to the systems involving actinides is limited because, at present, the parameters for actinide species that need to be determined by regression procedures with experimental data do not exist. As a result, reliable experimental data on the complexation of actinides in solution at elevated temperatures are still needed.

In addition to providing support to the safe management of nuclear wastes, the study of the complexation of actinides in solution at elevated temperatures could improve the fundamental understanding of the coordination chemistry of actinides as well. For example, the change in temperature could affect the solvent structure, its dielectric property and the energetics of the complexation.[9–11] Therefore, thermodynamic parameters over a range of temperatures could provide insight into the nature of the actinide complex and the solvent effect.

We have started investigations on the complexation of actinides and lanthanides with a series of mono- and polycarboxylic acids in solution at variable temperatures. These ligands either exist in the nuclear wastes or are of importance in waste processing or metal transport in the repository. This paper summarizes the results of the complexation of uranium(VI) with acetate from 25 to 70 °C. This system has been previously studied at 20 and 25 °C,[3,12–17] but not at elevated temperatures. Furthermore, due to the unavailability of techniques to characterize the coordination modes, little structural information was obtained on the complexes in solution in the earlier studies. Therefore, our objectives in this work are: (1) to extend the thermodynamic database for the complexation of uranium(VI) with acetate to elevated temperatures and help predict the chemical behavior of actinides in nuclear wastes; (2) to provide insight into the nature of the uranyl acetate complexes and the energetics of the complexation, and establish the coordination modes in the complexes, using an integrated approach of thermodynamic measurements and spectroscopic characterization. Thermodynamic parameters including formation constants, enthalpy and entropy were determined by potentiometry and calorimetry. Extended X-ray Absorption Fine Structure Spectroscopy (EXAFS) was used, in conjunction with the thermodynamic data, to establish the coordination modes in the complexes.

2 Results and discussion

2.1 Protonation of acetate

The acetate protonation constants at different temperatures were calculated from the data obtained by potentiometry. These constants were then used in the calculation of the enthalpies of protonation from the data obtained by calorimetry at the same temperature. The results are summarized in Table 1. The protonation constant and the enthalpy at 25 °C are in excellent agreement with the available values from the literature.[3,12]

As shown by the data in Table 1, the enthalpy of protonation of acetate is small (less than a few kJ mol^{-1}) and changes from exothermic (at 25–35 °C) to endothermic (at 45–70 °C), showing that the enthalpy term is unfavorable to the protonation at higher temperatures. Meanwhile, the entropy of protonation increases from 83 J K^{-1} mol^{-1} (25 °C) to 99 J K^{-1} mol^{-1} (70 °C), thus enhancing the protonation at higher temperatures. The increase in the entropy term ($T\Delta S$) is slightly larger than the increase in the enthalpy, resulting in a net increase in the protonation constant when the temperature is increased. The results from this work compare well with the previous results[5] of acetate protonation in 2.2 mol kg^{-1} $NaClO_4$ and agree with the

 DOI: 10.1039/b106642k

Table 1 Acetate protonation constants and corresponding thermodynamic parameters,[a] $I = 1.05$ mol kg^{-1} ($NaClO_4$)

T/°C	log $K_{H,M}$	log $K_{H,m}$	$-\Delta G_{H,m}$/kJ mol^{-1}	$\Delta H_{H,m}$/kJ mol^{-1}	$\Delta S_{H,m}$/J K^{-1} mol^{-1}
25	4.59 ± 0.01	4.62 ± 0.01	26.4	−1.63 ± 0.09	83 ± 1
	4.58 ± 0.03[b]			−1.4 ± 0.8[b]	84
35	4.62 ± 0.01	4.65 ± 0.01	27.4	−0.62 ± 0.03	87 ± 1
45	4.63 ± 0.01	4.66 ± 0.01	28.4	0.32 ± 0.03	90 ± 1
55	4.65 ± 0.02	4.68 ± 0.02	29.4	1.29 ± 0.03	94 ± 1
70	4.72 ± 0.02	4.75 ± 0.02	31.2	2.79 ± 0.16	99 ± 1

[a] The protonation constant $K_H = [HL]/([H^+][L^-])$, where L stands for acetate. $K_{H,M}$ and $K_{H,m}$ represent the protonation constants on the molarity and the molality scales, respectively. All error limits represent 3σ. [b] Refs. 3 and 12.

thermodynamic protonation constants predicted by Shock[8b] using a modified HKF equation of state (4.76, 4.79 and 4.85 at 25, 50 and 75 °C, respectively).

2.2 Complexation of uranyl with acetate

2.2.1 Formation constants and Gibbs free energy at 25 to 70 °C. Fig. 1 shows the potentiometric titration data for the uranyl acetate system at five different temperatures, in the form of $\bar{n}$ *vs.* log [L]. $\bar{n}$ is the average number of acetate ions bound to each uranyl as calculated by

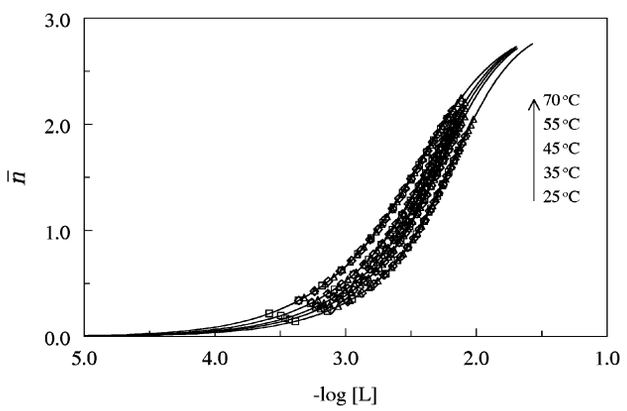

Fig. 1 Potentiometric titrations of the uranyl acetate system: The complex formation function ($\bar{n}$) as a function of log [L]. $I = 1.05$ mol kg^{-1} $NaClO_4$. Titrant: 0.994 M HAc/0.494 M NaAc. Initial cup volume: 40 mL. Initial cup solutions: (△) 5.680 mM $UO_2(ClO_4)_2$/6.023 mM $HClO_4$; (□) 9.655 mM $UO_2(ClO_4)_2$/10.24 mM $HClO_4$; (◇) 14.20 mM $UO_2(ClO_4)_2$/15.06 mM $HClO_4$. 50–70 data points were collected in each titration (the number of points in the figure is reduced for clarity).

$$\bar{n} = \{C_L - [L](1 + K_{H,M}[H^+])\}/C_U \quad (1)$$

where C_L and C_U are the concentrations of total acetate and total uranyl in solution and [L] is the concentration of free acetate. The best fit of the data by the Superquad program indicates that, under the experimental conditions, three successive uranyl acetate complexes form during the titration. The overall complexation reactions are represented by equilibrium (2).

$$UO_2^{2+} + j\,CH_3COO^- \rightleftharpoons UO_2(OOCCH_3)_j^{(2-j)+} \quad j = 1, 2, 3 \quad (2)$$

$$\beta_j = [UO_2(OOCCH_3)_j^{(2-j)+}]/([UO_2^{2+}][CH_3COO^-]^j) \quad (3)$$

The equilibrium constants and the corresponding Gibbs free energy of these reactions are calculated and given in Table 2. To show the goodness of the constants, simulated titration curves were calculated with them and plotted with the experimental data in Fig. 1. The consistency between the calculated curves and the experimental points indicates that the potentiometric titration data are accurately represented by the formation of the three successive uranyl acetate complexes.

In general, the overall formation constants in Table 2 (β_1, β_2 and β_3, eqn. (3)) increase as the temperature is elevated. However, it is more informative to discuss the temperature effect on the stepwise reactions:

$$UO_2(OOCCH_3)_{j-1}^{(2-j+1)+} + CH_3COO^- \rightleftharpoons UO_2(OOCCH_3)_j^{(2-j)+} \quad j = 1, 2, 3 \quad (4)$$

where the stepwise formation constants are related to the overall constants and expressed as

$$K_j = [UO_2(L)_j^{(2-j)+}]/([UO_2(L)_{j-1}^{(2-j+1)+}][L^-]) \quad (5)$$

where L stands for CH_3COO.

If we convert the overall constants into stepwise formation constants, it is found that only K_1 and K_2 increase with the temperature (from 25 to 70 °C, $\Delta\log K_1 \approx 0.4$, $\Delta\log K_2 \approx 0.5$), while K_3 seems insensitive to the change in temperature (from 25 to 70 °C, K_3 fluctuates and $\Delta\log K_3$ is comparable to the experimental uncertainties). These trends could be rationalized with a Born-type electrostatic model as follows.

As discussed in previous publications, the effect of temperature on the formation constants of the complexes between a hard acid (*e.g.*, actinide and lanthanide cations) and a hard base (*e.g.*, oxygen donor ligands such as acetate) could be interpreted with an electrostatic model.[5,18–21] Combining a modified Born equation[5,21] and the empirical expression for the dielectric constant of water[22,23] ($\varepsilon = \varepsilon_0\exp(-T/\theta)$, where $\varepsilon_o = 305.7$; $\theta = 219$ K), the temperature coefficient of the complexation constants is expressed as

$$\partial(\log\beta)/\partial T = Ne^2Z_1Z_2/(0.2303Rd_{12})(1/T - 1/\theta)/(\varepsilon T) \quad (6)$$

where the symbols are explained in ref. 21. Since θ is far below the freezing point of water, T is always higher than θ in the whole accessible temperature range of an aqueous solution. As a result, $(1/T - 1/\theta)$ is always negative. Thus, eqn. (4) predicts the following temperature dependencies of the complexation between species 1 and 2: $\partial(\log\beta)/\partial T > 0$ if $Z_1Z_2 < 0$; $\partial(\log\beta)/\partial T < 0$ if $Z_1Z_2 > 0$; $\partial(\log\beta)/\partial T = 0$ if $Z_1Z_2 = 0$. These predictions are in good agreement with the experimental data on uranyl acetate in the temperature range of 25 to 70 °C: the stepwise constants K_1 and K_2 increase significantly with the temperature (for the first two steps, $Z_1Z_2 < 0$). On the other hand, K_3 is insensitive to the temperature change (for the third step, $Z_1Z_2 \approx 0$). It should be emphasized that the discussions based on the electrostatic model are qualitative. Though the complexation between a hard acid and a hard base is predominantly electrostatic, other interactions (*e.g.*, covalent interaction) could have minor contributions. Besides, electrostatic interactions may not be completely ignored in the complexation involving a neutral species due to the charge distribution and/or inductive effect. More detailed and quantitative discussions on this subject will become feasible when we extend the variable temperature studies to more diversified complex systems.

Table 2 Formation constants and corresponding thermodynamic parameters[a] for uranyl acetate complexation, $I = 1.05$ mol kg^{-1} ($NaClO_4$)

	T/°C	$\log \beta_{j,M}$	$\log \beta_{j,m}$	$-\Delta G_m$/kJ mol^{-1}	ΔH_m/kJ mol^{-1}	ΔS_m/J K^{-1} mol^{-1}
$UO_2^{2+} + Ac^- \rightleftharpoons [UO_2Ac]^+$	25	2.58 ± 0.03	2.61 ± 0.03	14.9	10.6 ± 0.8	86 ± 3
		2.44 ± 0.02[b]			11.3 ± 0.8[b]	85[b]
	35	2.67 ± 0.02	2.70 ± 0.02	15.9	11.8 ± 0.5	90 ± 2
	45	2.74 ± 0.03	2.77 ± 0.03	16.9	13.0 ± 0.6	94 ± 2
	55	2.85 ± 0.02	2.88 ± 0.02	18.1	14.3 ± 0.5	99 ± 2
	70	2.98 ± 0.05	3.01 ± 0.05	19.8	15.4 ± 0.7	102 ± 3
$UO_2^{2+} + 2Ac^- \rightleftharpoons [UO_2Ac_2]$	25	4.37 ± 0.14	4.43 ± 0.14	25.3	20 ± 3	152 ± 13
		4.42 ± 0.04[b]			19 ± 2[b]	149[b]
	35	4.60 ± 0.08	4.66 ± 0.08	27.5	21 ± 2	157 ± 8
	45	4.76 ± 0.10	4.82 ± 0.10	29.4	22 ± 2	161 ± 8
	55	4.94 ± 0.06	5.00 ± 0.06	31.4	24 ± 1	169 ± 4
	70	5.27 ± 0.09	5.33 ± 0.09	35.0	27 ± 1	181 ± 5
$UO_2^{2+} + 3Ac^- \rightleftharpoons [UO_2Ac_3]^-$	25	6.86 ± 0.04	6.95 ± 0.04	39.7	17.5 ± 0.6	192 ± 3
		6.43 ± 0.09[b]			16 ± 2[b]	179[b]
	35	7.11 ± 0.03	7.20 ± 0.03	42.5	18.8 ± 0.3	199 ± 2
	45	7.23 ± 0.04	7.32 ± 0.04	44.6	20.8 ± 0.3	206 ± 2
	55	7.38 ± 0.03	7.47 ± 0.03	46.9	22.8 ± 0.3	212 ± 2
	70	7.62 ± 0.06	7.71 ± 0.06	50.6	24.6 ± 0.4	219 ± 2

[a] $\beta_{j,M} = [ML_j]/([M][L]^j)$, where M and L stand for uranium(VI) and acetate, respectively. All error limits represent 3σ. [b] Refs. 3 and 12.

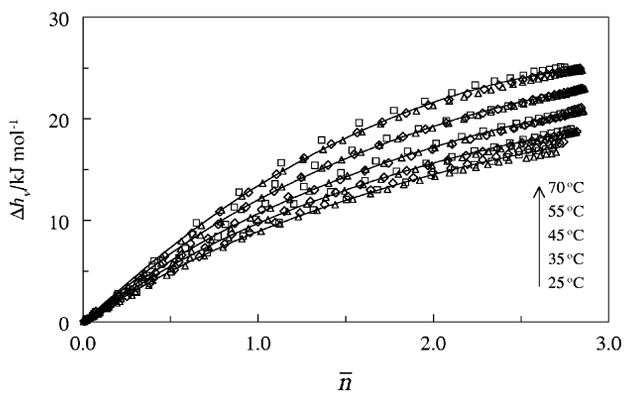

Fig. 2 Calorimetric titrations of the uranyl acetate system: Total enthalpy changes per mole of uranium as a function of $\bar{n}$. $I = 1.05$ mol kg^{-1} $NaClO_4$. Titrant: 0.994 M HAc/0.494 M NaAc. Initial cup volume: 20 mL. Initial cup solutions: (△) 5.680 mM $UO_2(ClO_4)_2$/6.023 mM $HClO_4$; (□) 9.655 mM $UO_2(ClO_4)_2$/10.24 mM $HClO_4$; (◇) 14.20 mM $UO_2(ClO_4)_2$/15.06 mM $HClO_4$. 50–70 data points were collected in each titration (the number of points in the figure is reduced for clarity).

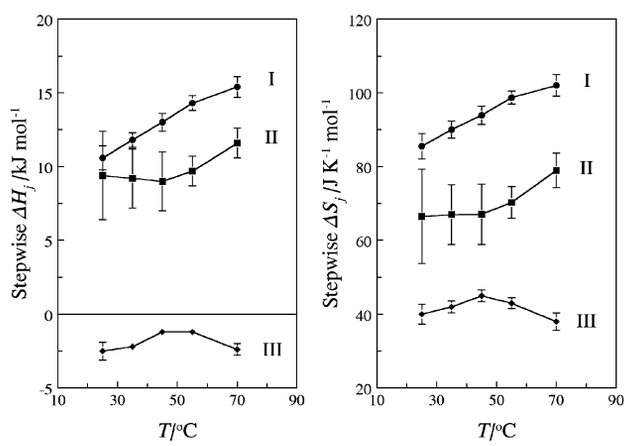

Fig. 3 Stepwise enthalpy and entropy of uranyl acetate complexation as functions of temperature. $I = 1.05$ mol kg^{-1} $NaClO_4$.

2.2.2 Enthalpy and entropy of complexation at 25 to 70 °C. The experimental data of the calorimetric titrations are shown in Fig. 2, in the form of Δh_v *vs.* $\bar{n}$. Values of $\bar{n}$ were calculated using the formation constants obtained by potentiometry and the analytical concentrations of uranium, H^+ and acetate at each step of the titration. In the calculation of Δh_v, the heat due to the protonation or deprotonation of acetate has been subtracted from the total reaction heat. From these data, the enthalpies and entropies of complexation were calculated and summarized in Table 2. Using the enthalpies and formation constants in Table 2, curves simulating the calorimetric titrations were calculated and shown in Fig. 2. The excellent agreement between the curves and the experimental points confirms the mutual consistency of the calorimetric and potentiometric data on the complexation as well as the reliability of the data on protonation.

Though the enthalpy term becomes more unfavorable to the complexation as the temperature is elevated, the complexes are more stable at higher temperatures because of the increasingly more positive entropy of complexation (Table 2). This is similar to the entropy-driven complexation between neodymium(III) and acetate,[5] and can be related to the perturbation of the solvent structure by thermal motions at higher temperatures. This effect has been discussed elsewhere.[5,9,10]

Stepwise, the contributions of each complexation to the overall enthalpy and entropy are different, as shown in Fig. 3. The following trends in the enthalpy and entropy of the stepwise complex formation can be summarized. (1) The first two steps are endothermic but the third is exothermic and the enthalpy change decreases in the order: ΔH_1 (10–15 kJ mol^{-1}) > ΔH_2 (8–12 kJ mol^{-1}) ⩾ ΔH_3 (≈ −2 kJ mol^{-1}). (2) The entropy change becomes smaller in the order: ΔS_1 (85–102 J K^{-1} mol^{-1}) > ΔS_2 (64–79 J K^{-1} mol^{-1}) > ΔS_3 (30–45 J K^{-1} mol^{-1}) and ΔS_3 is less than 50% of ΔS_1. As pointed out by Ahrland,[24] the changes in thermodynamic parameters can be related to the changes of the coordination modes in the complexes. The trends observed in this work may provide insight into the coordination modes of acetate in the complexes and the changes in the primary hydration sphere as well as in the bulk solvent in each complexation step. Further discussions are made in conjunction with the structural information obtained by EXAFS.

2.2.3 Characterization of uranyl acetate species in solution by EXAFS. The background-subtracted uranium L3-edge EXAFS spectra and corresponding Fourier transforms are shown in Fig. 4. The fitting parameters are summarized in Table 3. In the Fourier transforms for all the samples, solid and solution, a prominent feature at ≈1.8 Å (after correction for the phase shift) is present, representing the two axial oxygens in the uranyl cations. In the following discussions, this feature is ignored in order to focus on the coordination of equatorial oxygens and carbons.

In the crystal structure of uranyl acetate dihydrate (Fig. 5a) determined by X-ray crystallography,[25] one acetate is bidentate

Table 3 Best fit parameters for uranium L3-edge EXAFS

Samples	Shell	R^a/Å	N^a	σ,^{b}/Å	ΔE_0/eV	R_{crys} ^{c}/Å
$UO_2(Ac)_2 \cdot 2H_2O$ (crystal)	$U–O_{ax}$	1.78	2.0	0.0452	−14.89	1.74, 1.76
	$U–O_{eq1}$	2.36	2.8	0.0379	−14.89	2.37, 2.34
	$U–O_{eq2}$	2.49	1.8	0.0143	−14.89	2.45
$Na[UO_2(Ac)_3]$ (crystal)	$U–O_{ax}$	1.78	1.7	0.0187	−14.76	1.76
	$U–O_{eq}$	2.48	6.4	0.0776	−14.76	2.464
	U–C	2.88	2.8	0.0499	−14.76	2.85
Solution I	$U–O_{ax}$	1.78	2.0	0.0411	−14.48	
1 : 1 Uranyl/Ac, pH = 2.84	$U–O_{eq1}$	2.38	4.0	0.0703	−14.48	
	$U–O_{eq2}$	2.50	2.0	0.0920	−14.48	
	U–C	2.91	1.3	0.0500	−14.48	
Solution II	$U–O_{ax}$	1.78	2.0	0.0370	−12.45	
Mixture, pH = 3.46	$U–O_{eq}$	2.42	5.9	0.0888	−12.45	
	U–C	2.90	2.2	0.0500	−12.45	
Solution III	$U–O_{ax}$	1.78	2.0	0.0344	−12.37	
1 : 3 Uranyl/Ac, pH = 3.85	$U–O_{eq1}$	2.34	1.9	0.0533	−12.37	
	$U–O_{eq2}$	2.48	4.1	0.0482	−12.37	
	U–C	2.87	2.1	0.0500	−12.37	
Solution IV	$U–O_{ax}$	1.78	2.0	0.0390	−12.51	
1 : 3 Uranyl/Ac, pH = 4.5	$U–O_{eq1}$	2.32	3.1	0.0736	−12.51	
	$U–O_{eq2}$	2.47	2.9	0.0601	−12.51	
	U–C	2.87	1.0	0.0500	−12.51	

^{a} The 95% confidence limits for the bond lengths (R) and coordination numbers (N) for each shell are: $U–O_{ax}$, 0.01 Å and ±15%; $U–O_{eq}$, 0.02 Å and ±25%; U–C, 0.02 Å and ±25%, respectively. ^{b} σ is the EXAFS Debye–Waller term that accounts for the effects of thermal and static disorder through damping of the EXAFS oscillations by the factor $\exp(-2k^2\sigma^2)$. ^{c} Refs. 25 and 27.

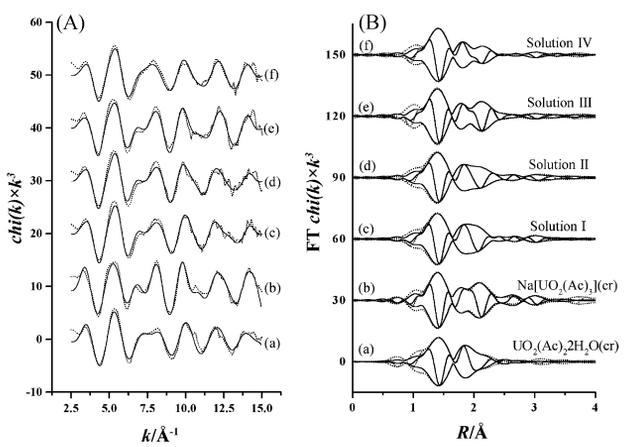

Fig. 4 Experimental (dotted lines) and fitted (solid lines) uranium L3-edge EXAFS spectra (A) and associated Fourier transforms (B). The distance (R) is not corrected for the phase shift. (a) $UO_2(OOCCH_3)_2 \cdot 2H_2O$(crystal). (b) $Na[UO_2(OOCCH_3)_3]$(crystal). (c) Solution I. (d) Solution II. (e) Solution III. (f) Solution IV (see Table 3 for the compositions of solutions I–IV).

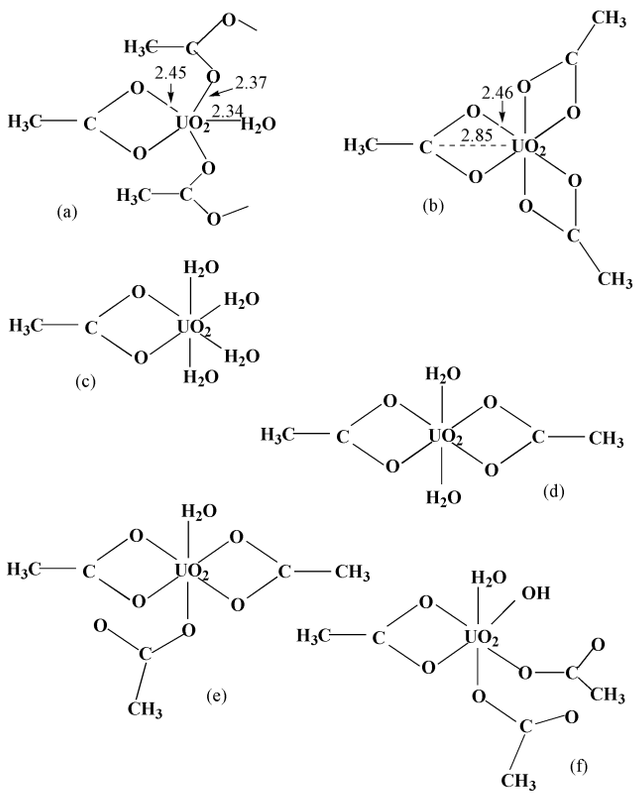

Fig. 5 Solid structures of uranyl acetate compounds and proposed structures of uranyl acetate complexes in solution. (a) $UO_2(OOCCH_3)_2 \cdot 2H_2O$(crystal).[25] (b) $Na[UO_2(OOCCH_3)_3]$(crystal).[27] (c) $UO_2(OOCCH_3)^+$(aq.). (d) $UO_2(OOCCH_3)_2^0$(aq.). (e) $UO_2(OOCCH_3)_3^-$(aq.). (f) $UO_2OH(OOCCH_3)_3^{2-}$(aq.).

(two oxygens, $R_{U–O}$ = 2.45 Å) and two acetates are unidentate to uranium (two oxygens, $R_{U–O}$ = 2.37 Å). The water molecule is at a distance of $R_{U–O}$ = 2.34 Å. Consistent parameters were obtained by EXAFS — two oxygens at 2.49 Å and three oxygens at 2.36 Å (the two oxygens from the unidentate acetates and the oxygen from water are not distinguished). In the crystal structure of sodium uranyl triacetate[26,27] (Fig. 5b), all the three acetates are bidentate. In this case, the $U–O_{eq}$ distance is 2.46 Å and the U–C distance is 2.85 Å. Again, the EXAFS best fit agrees well with the crystallographic data, showing six equatorial oxygens at 2.48 Å and three carbons at 2.88 Å. These data, consistent with the observations by Denecke *et al.*,[28] show that the bidentate and unidentate acetate can be differentiated by two features: (1) the $R_{U–O}$ is longer in the former (≈2.45–2.48 Å) than in the latter (≈2.35 Å); (2) the $R_{U–C}$ in the former is ≈2.85–2.88 Å, easily identified by EXAFS. However, detecting the carbon in a unidentate acetate may be difficult due to its longer distance ($R_{U–C}$ 3.5 Å) and the overlap of oscillations resulting from the U–C single scattering and the linear O=U=O multiple scattering (1.78 × 2 Å).

The Fourier transforms of the EXAFS spectra for the four solutions (Fig. 4B, curves c–f) show systematic changes in the region around 2 Å (before correction for the phase shift). This is the region that accounts for the scattering interactions with equatorial oxygen and carbon atoms. From the 1 : 1 uranyl acetate complex (solution I, curve c), through the mixture (solution II, curve d), to the 1 : 3 complex (solution III, curve e), the broad peak at ≈2 Å splits into two at 1.8 and 2.15 Å, respectively. From curve c to curve e, the feature at 2.15 Å becomes

more significant, suggesting that more oxygens and/or carbons are found in a distant shell in the 1 : 3 complex than in the 1 : 1 complex. These spectra were fit with the standard paths calculated from the reference compounds.

The best fit of the EXAFS data for the 1 : 1 uranyl acetate complex (solution I, curve c of Fig. 4B) suggests that the acetate is bidentate to uranium (two oxygens at 2.50 Å and one carbon at 2.91 Å), corresponding to the structure shown in Fig. 5c. The best fit for solution II (curve d of Fig. 4B) shows two carbons at 2.90 Å, implying that there are two bidentate acetates per uranium. However, since no single species is dominant in this solution and the EXAFS results represent the average for all the species, we cannot unambiguously assign the structure of the 1 : 2 complex based on the EXAFS data. There have been arguments about the coordination modes in the 1 : 2 uranyl acetate complex.[29–32] Studies by Kakihana *et al.*[29] (IR and ^{13}C NMR) show that the two acetates are bidentate, while the results from Quilès and Burneau[31] (IR and Raman) suggest one bidentate and one "pseudo-bridging" acetate. Our data are inconclusive in distinguishing the two models. As a result, the structure of the 1 : 2 complex shown in Fig. 5d is tentatively proposed.

For the solution of the 1 : 3 complex at pH 3.85 (solution III, curve e of Fig. 4B), the best fit indicates that two acetates are bidentate (four oxygens at 2.48 Å and two carbons at 2.87 Å) and the third acetate is unidentate (the oxygen is at 2.34 Å and indistinguishable from the oxygen of water). These data indicate that the structure of the 1 : 3 complex in solution (Fig. 5e) differs from that in the crystal (Fig. 5b) and that different coordination modes (bidentate and unidentate) are involved in the formation of the complexes in solution as the thermodynamic results suggest.

Based on the structural information on the uranyl acetate complexes in solution, the thermodynamic trends discussed in section 2.2 (Fig. 3) can be rationalized in terms of the perturbation by the complex formation in the primary hydration sphere and the bulk structure of water. Since the degree of charge neutralization decreases as the stepwise complexation progresses, the energy required for restructuring the bulk solvent is expected to become less in the successive steps. Thus the stepwise enthalpy change decreases in the order: $\Delta H_1 > \Delta H_2 > \Delta H_3$. Furthermore, the unidentate acetate in the third complex (Fig. 5e) replaces only one water molecule in the primary hydration sphere so that it requires less desolvation energy than a bidentate coordination. Consequently, the enthalpy change in the third step is much less than the first two and, in this particular case, the stepwise formation of the third complex becomes exothermic.

Similarly, the trend in entropy can be interpreted based on the structural information of the uranyl acetate complexes in solution. In general, the entropy change upon the complexation consists of ΔS_t (translational), ΔS_r (rotational) and ΔS_c (conformational). The change in vibrational entropy (ΔS_v) can usually be neglected. Quantitative evaluation of the entropy effect in complexation is difficult because the quantities ΔS_t, ΔS_r and ΔS_c are not easy to assess[10] and the information on the solvation of the ligand is rarely available. However, integration of the thermodynamic data and structural information obtained in this work allows qualitative discussions. A larger gain in the translational entropy is certainly expected for a bidentate complex (steps 1 and 2) than a unidentate complex (step 3), because the former replaces more water molecules from the primary hydration sphere. Besides, the higher degree of charge neutralization in step 1 and then step 2 causes a larger net increase in the disorder of the bulk water. In addition, it is reasonable to assume that the structuring effect of a unidentate acetate on the bulk water could be stronger than a bidentate acetate because the former is more capable of forming hydrogen bonds with bulk water due to its "free" oxygen (Fig. 5e). The combination of all these effects results in a much smaller ΔS_3 and the decreasing order of the stepwise entropy changes: $\Delta S_1 > \Delta S_2 > \Delta S_3$.

Interestingly, the EXAFS data show that, when the pH of the solution of the 1 : 3 complex is increased from 3.85 to 4.5, only one carbon is identified at 2.87 Å (solution IV, curve f of Fig. 4B, Table 3). This may suggest that only one acetate remains in the bidentate mode and the other acetate (bidentate in solution III where the pH is 3.85) is "broken out" to become unidentate so as to accommodate a hydroxyl group in the equatorial plane (Fig. 5f). However, further experimental evidence is needed to confirm the presence of this mixed uranyl–hydroxy–acetate complex.

3 Conclusions

In the temperature range from 25 and 70 °C, three uranyl acetate complexes (1 : 1, 1 : 2 and 1 : 3) were identified by potentiometry and calorimetry. The increase in temperature greatly enhances the stepwise formation of the first and the second complexes but has an insignificant effect on the third step. A Born-type electrostatic model provides satisfactory explanation for these effects.

The stepwise thermodynamic parameters of the third complex are significantly different from those of the first two steps: ΔH_3 is negative while ΔH_1 and ΔH_2 are positive; ΔS_3 is less than 50% of ΔS_1. This difference is rationalized by the hypothesis that, in the 1 : 3 complex, the third acetate ligand is in a different coordination mode from the other two acetate ligands. EXAFS data for the solution species support such a hypothesis and help to interpret the thermodynamic data.

4 Experimental

4.1 Chemicals

All chemicals were reagent grade or higher. Distilled water was used in preparations of all the solutions. The stock solution of uranyl perchlorate was prepared by dissolving uranium trioxide (UO_3) in perchloric acid (Aldrich, 70%). The amount of perchloric acid was in excess with respect to the stoichiometric ratio of 2 : 1 (C_{HClO_4} : C_U) to avoid the hydrolysis of uranium. The concentrations of uranium and perchloric acid in the stock solution were determined by EDTA titration complexometry[33] and fluorimetry,[34] and Gran's potentiometric method,[35] respectively. Sodium hydroxide solutions, free from carbonate, were standardized against 1.005 mol dm^{-3} hydrochloric acid (Aldrich, ACS volumetric standard). The standardized sodium hydroxide solution was in turn used to determine the concentrations of perchloric acid and acetic acid by potentiometry. Buffer solutions of sodium acetate/acetic acid were prepared by adding calculated amounts of sodium hydroxide into solutions of acetic acid. The ionic strength of all the solutions used in potentiometry and calorimetry was adjusted to 1.0 mol dm^{-3} at 25 °C by adding appropriate amounts of sodium perchlorate as the background electrolyte.

4.2 Potentiometry

Potentiometric titrations were conducted to determine the protonation constants of acetate and the stability constants of uranyl acetate complexes at 25, 35, 45, 55, and 70 °C. Details of the titration setup have been provided elsewhere.[5] Both the titration cup and the lid were water-jacketed and maintained at the desired temperatures by water circulating from a constant temperature bath. It is important, especially for the titrations at temperatures higher than the ambient, to maintain the lid at the same temperature as the cup (and the solution in the cup) to avoid water condensation underneath the lid. Electromotive force (emf) was measured with a Metrohm pH meter (Model 713) equipped with a Ross combination pH electrode (Orion Model 8102). This electrode is workable for pH measurements

in a temperature range up to 100 °C. The original electrode filling solution (3.0 mol dm^{-3} potassium chloride) was replaced with 1.0 mol dm^{-3} sodium chloride to avoid clogging of the electrode frit glass septum by precipitation of $KClO_4$.

Prior to each protonation or complexation titration, the electrode was calibrated by an acid–base titration (using the standardized perchloric acid and sodium hydroxide solutions) at the desired temperature so that hydrogen ion concentrations could be calculated from the emf readings in the subsequent titration. All the emf data were corrected for a small contribution from the contact junction potential of the hydrogen ion, $\Delta E_{j,H^+}$. Corrections for the contact junction potential of the hydroxide ion were not necessary in these experiments. The emf data were collected at time intervals determined by the data collection criterion, *i.e.*, the drift of emf (ΔE) is less than 0.1 mV for 1 min.[36] Usually three or more titrations with different metal or ligand concentrations were conducted for each system.

In the studies of acetate protonation, the titrations were conducted in two ways: (1) a buffered acetate solution (0.1 mol dm^{-3}) was placed in the cup and titrated with perchloric acid; (2) an acetic acid solution (0.1 mol dm^{-3}) was placed in the cup and titrated with sodium hydroxide. In the studies of uranyl acetate complexation, the titrations were conducted with uranyl perchlorate (0.006–0.015 mol dm^{-3}) in the cup and titrated with buffered acetate solution. In all the titrations, the initial volume of the cup solutions was always 40 cm^3 at 25 °C. Multiple runs were conducted at each temperature with different uranyl concentrations. The protonation constants of acetate, $K_{H,M}$, and the formation constants of uranyl acetate complexes, $\beta_{j,M}$, on the molarity scale were calculated with the program Superquad.[37]

To compare the results at different temperatures, the constants calculated on the molarity scale were converted to the values on the molality scale as suggested by Grenthe and Ots.[38] Since the protonation and complex formation constants at variable temperatures are obtained from the potentiometric data referring to the additions, volumes, and concentrations at 25 °C, such conversion can be accomplished by the following equations:

$$K_{H,m} = K_{H,M} \times d_{298} \quad (7)$$

$$\beta_{j,m} = \beta_{j,M} \times (d_{298})^j \quad (8)$$

Where d_{298} (= 1.073 g cm^{-3}) is the density of 1.0 mol dm^{-3} sodium perchlorate in water at 25 °C.[39] This solution, equivalent to a solution of 1.05 mol kg^{-1} $NaClO_4$, is chosen as the reference solution for the calculation of the stability constants on the molality scale.

4.3 Calorimetry

Calorimetry was used to determine the enthalpy changes of acetate protonation and complexation with uranium(VI). The titrations were conducted with an isoperibol solution calorimeter (Model ISC-4285, Calorimetry Sciences Corp.) controlled by a computer. The titration assembly includes a 25 cm^3 reaction vessel, a thermistor, a calibration heater and a glass stirrer driven by an electric motor. The assembly was immersed in a high precision water bath (Hart Scientific), which has a volume of 25 dm^3 and maintains the temperature to ±0.001 °C. The titrant was delivered into the reaction vessel through a titrant tube from a syringe, which was also immersed in the water bath. The syringe was driven by a precision stepper motor that guarantees accurate delivery of the titrant at specific rates. The mass of the titrant solution delivered was calculated from the volume of the addition and the density of the reference solution (1.05 mol kg^{-1} $NaClO_4$) at the experimental temperature.[39] The performance of the calorimeter was tested by measuring the enthalpy of protonation of 2-bis(2-hydroxyethyl)amino-2-hydroxymethylpropan-1,3-diol (BIS–TRIS) at different temperatures. The results are 29.1 ± 0.3 kJ mol^{-1} at 45 °C and −29.3 ± 0.3 kJ mol^{-1} at 70 °C, which compare very well with those in the literature (−28.4 ± 0.3 kJ mol^{-1} at 45 °C and −29.3 ± 0.2 kJ mol^{-1} at 70 °C).[40]

The initial cup solutions and the titrants in the calorimetric titrations were similar to those in the potentiometric titrations described previously, except that the initial volume of the cup solution was 20 cm^3 at 25 °C. For each titration run, n experimental values of the total heat produced in the reaction vessel ($Q_{ex,j}$, j = 1 to n) were calculated as a function of the mass of the added titrant. These values were corrected for the heat of dilution of the titrant ($Q_{dil,j}$), which was determined in separate runs. The net reaction heat at the j-th point ($Q_{r,j}$) was obtained from the difference: $Q_{r,j} = Q_{ex,j} - Q_{dil,j}$. The quantity Δh_v, the total heat per mole of proton (in protonation titrations) or uranium (in complexation titrations), was calculated by dividing the net reaction heat with the number of moles of protons or uranium in the calorimeter vessel. The enthalpy changes of the acetate protonation and uranyl acetate complexation were calculated with the computer program Letagrop[41] with Δh_v as the error-carrying variable.

4.4 Extended X-ray absorption fine structure (EXAFS) spectroscopy

EXAFS experiments were conducted to obtain structural information on the uranyl acetate complexes in four solutions (I to IV). All the solutions contained 18.94 mM uranium(VI) perchlorate and 18.94 mM perchloric acid. The concentrations of acetic acid/sodium acetate buffer in the solutions were 53 mM/26 mM (solution I), 122 mM/61 mM (solution II) and 211 mM/105 mM (solutions III and IV). In solution IV, a small amount of sodium hydroxide was added to raise the pH from 3.85 (solution III) to 4.5 (solution IV). Speciation calculations indicate that the 1 : 1 complex, $UO_2(OOCCH_3)^+$, is dominant in solution I, and the 1 : 3 complex, $UO_2(OOCCH_3)_3^-$, is dominant in solution III (>90%). Solution II represents a mixture of 1 : 1, 1 : 2 and 1 : 3 complexes without a single dominant species. Approximately 2 cm^3 of the solution was sealed in a polyethylene tube (5 mm i.d.) and mounted on an aluminium sample positioner with Scotch tape for the EXAFS experiments.

EXAFS spectra of two reference compounds, uranyl acetate dihydrate ($UO_2(OOCCH_3)_2 \cdot 2H_2O$) and sodium uranyl triacetate ($Na[UO_2(OOCCH_3)_3]$), were also collected. The solid samples were prepared by mixing appropriate amounts of the compounds with boron nitride and loading the mixture to aluminium holders with a rectangular opening of 20 mm (L) × 2 mm (W) and a thickness of 0.5–1 mm. The holders were mounted on the sample positioner with Scotch tape.

Uranium L3-edge EXAFS spectra were collected at the Stanford Synchrotron Radiation Laboratory (SSRL) on wiggler beamline 4–1 under normal ring operating conditions (3.0 GeV, 50–100 mA). Energy scans of the polychromatic X-ray beam were obtained using a Si(220) double-crystal monochromator. The vertical slit width was 0.5 mm, which reduced the effects of beam instabilities and monochromator glitches while providing ample photon flux. The higher order harmonic content of the beam was reduced by detuning the crystals in the monochromator so that the incident flux was reduced to 50% of its maximum at the scan ending energy. The EXAFS data were collected in the transmission mode using argon-filled ionization chambers, up to $k_{max} \approx 15$ $Å^{-1}$, which allowed the shell resolution to be about 0.1 Å since $\Delta R \geq \pi/(2k_{max})$.[42] Three or more scans were performed for each sample. Energy calibration was based on assigning the first inflection point of the absorption edge for uranium dioxide (UO_2) to 17166 eV. The EXAFS

spectra were fit with the *R*-space X-ray Absorption Package (RSXAP),[43] using parameterized phase and amplitude functions generated by the program FEFF7[44] with the crystal structures of uranyl acetate dihydrate and sodium uranyl triacetate. Standard scattering paths were calculated from the crystal structures.[25–27] In the data analysis, full cluster multiple scattering calculations were tried, but were found to have no influence on the best fit parameters and the overall goodness of the fit. As a result, only the following relevant paths were included in the calculation: the single scattering interactions of U–O_{ax} (axial oxygen), U–O_{eq} (equatorial oxygen) and U–C, and the multiple scattering of O=U=O (axial oxygens).

Acknowledgements

This work was supported by the Director, Office of Science, Office of Basic Energy Sciences, Division of Chemical Sciences, and by the Assistant Secretary for Environmental Management under U.S. Department of Energy contract no. DE-AC03-76SF0098 at Lawrence Berkeley National Laboratory. The EXAFS experiments were conducted at SSRL, which is operated by the Department of Energy, Division of Chemical Sciences. The authors thank the colleagues at the Glenn T. Seaborg Center, Lawrence Berkeley National Laboratory, Drs. C. W. Booth and W. W. Lukens, Jr. in particular, for the help with the EXAFS and crystallography analyses.

References

1 DOE, *Estimating the Cold War Mortgage: The 1995 Baseline Environmental Management Report*, DOE/EM-0232, US Department of Energy, Washington DC, 1995.
2 J. M. Cruse, R. L. Gilchrist, *Developing Waste Disposal Options in the Underground Storage Tank-Integrated Demonstration Program*, in *Global 93, Future Nuclear Systems: Emerging Fuel Cycles and Waste Disposal Options*, American Nuclear Society, La Grange Park, IL, 1993, p. 1376.
3 A. E. Martell and R. M. Smith, *Critical Stability Constants*, Plenum Press, New York, 1989, vol. 6.
4 P. W. Atkins, *Physical Chemistry*, 6th edn., W. H. Freeman & Co., New York, 1997.
5 P. Zanonato, P. Di Bernardo, A. Bismondo, L. Rao and G. R. Choppin, *J. Solution Chem.*, 2001, **30**, 1–18.
6 (*a*) H. C. Helgeson and D. H. Kirkham, *Am. J. Sci.*, 1974, **274**, 1199–1261; (*b*) H. C. Helgeson and D. H. Kirkham, *Am. J. Sci.*, 1976, **276**, 97–240; (*c*) H. C. Helgeson, D. H. Kirkham and G. C. Flowers, *Am. J. Sci.*, 1981, **281**, 1249–1493; (*d*) H. C. Helgeson, in *Chemistry and Geochemistry of Solutions at High Temperatures and Pressures, Physics and Chemistry of the Earth*, Eds. D. T. Rickard and F. E. Wickman, Pergamon Press, Oxford, 1981, vol. 13 & 14, pp. 133–177.
7 J. C. Tanger and H. C. Helgeson, *Am. J. Sci.*, 1988, **288**, 19–98.
8 (*a*) E. L. Shock, *Geochim. Cosmochim. Acta*, 1993, **57**, 4899–4922; (*b*) E. L. Shock, *Am. J. Sci.*, 1995, **295**, 496–580; (*c*) E. L. Shock, D. C. Sassani, M. Willis and D. A. Sverjensky, *Geochim. Cosmochim. Acta*, 1997, **61**, 907–950; (*d*) E. L. Shock, E. H. Oelker, J. W. Johanson, D. A. Sverjensky and H. C. Helgeson, *J. Chem. Soc., Faraday Trans. I*, 1992, **88**, 803–826.
9 T. M. Seward, *Metal Complex formation in aqueous solutions at elevated temperatures and pressures*, in *Chemistry and Geochemistry of Solutions at High Temperatures and Pressures, Physics and Chemistry of the Earth*, Eds. D. T. Rickard and F. E. Wickman, Pergamon Press, Oxford, 1981, vol. 13 & 14, pp. 113–128.
10 G. Schwarzenbach, *Interpretation of solution stabilities of metal complexes*, in *Proceedings of Summer School for Stability Constants*, 1st edn., Scientific Eds. P. Paoletti, R. Barbucci and L. Fabbrizzi, University of Florence, Italy, 1977, pp. 151–181.
11 E. N. Rizkalla and G. R. Choppin, *Lanthanides and Actinides Hydration and Hydrolysis*, in *Handbook on the Physics and Chemistry of Rare Earths, Vol. 18 – Lanthanides/Actinides: Chemistry*, Eds. K. A. Gschneider, Jr., L. Eyring, G. R. Choppin and G. H. Lander, Elsevier Science B. V., New York, 1994.
12 R. Portanova, P. Di Bernardo, A. Cassol, E. Tondello and L. Magon, *Inorg. Chim. Acta*, 1974, **8**, 233.
13 S. Ahrland and l. Kullberg, *Acta Chem. Scand.*, 1971, **25**, 3677.
14 C. Miyake and H. W. Nurnberg, *J. Inorg. Nucl. Chem.*, 1967, **29**, 2411.
15 F. I. Kalili, G. R. Choppin and E. N. Rizkalla, *Inorg. Chim. Acta*, 1988, **143**, 131.
16 I. Feldman and L. Koval, *Inorg. Chem.*, 1963, **2**, 145.
17 S. Ahrland, *Acta Chem. Scand.*, 1951, **5**, 199.
18 V. M. Born, *Z. Phys.*, 1920, **1**, 45–48.
19 R. Münze, *J. Inorg. Nucl. Chem.*, 1972, **34**, 661–668.
20 G. R. Choppin and L. Rao, *Radiochim. Acta*, 1984, **37**, 143–146.
21 G. R. Choppin and P. J. Unrein, *Thermodynamic Study of Actinide Fluoride Complexation*, in *Transplutonium Elements*, Eds. W. Muller and R. Lindner, North-Holland Publishing Company, Amsterdam, 1976.
22 R. W. Gurney, *Ionic Processes in Solution*, McGraw-Hill, New York, 1953.
23 J. Wyman and E. N. Ingalls, *J. Am. Chem. Soc.*, 1938, **60**, 1182–1184.
24 S. Arhland, *Solvation and Complex formation in Protic and Aprotic Solvents*, in *The Chemistry of Nonaqueous Solvents*, Ed. J. J. Lagowsky, Academic Press, New York, 1978, pp. 1–62.
25 D. M. Howatson and B. Morosin, *J. Inorg. Nucl. Chem.*, 1975, **37**, 1933–1935.
26 A. Zalkin, H. Ruben and D. H. Templeton, *Acta Crystallogr., Sect. B*, 1982, **38**, 610–612.
27 D. H. Templeton, A. Zalkin, H. Ruben and L. K. Templeton, *Acta Crystallogr., Sect. C*, 1985, **41**, 1439–1441.
28 M. A. Denecke, T. Reich, S. Pompe, M. Bubner, K. H. Heise, H. itsche, P. G. Allen, J. J. Bucher, N. M. Edelstein and D. K. Shuh, *J. Phys. IV*, 1997, **7**, 637–638.
29 M. Kakihana, T. Nagumo, M. Okamoto and H. Kakihana, *J. Phys. Chem.*, 1987, **91**, 6128–6136.
30 C. Nguyen-Trung, G. M. Begun and D. A. Palmer, *Inorg. Chem.*, 1992, **31**, 5280–5287.
31 F. Quilès and A. Burneau, *Vibr. Spectrosc.*, 1998, **18**, 61–75.
32 M. Nara, H. Torii and M. Tasumi, *J. Phys. Chem.*, 1996, **100**, 19812–19817.
33 J. A. Dean, *Analytical Chemistry Handbook*, McGraw-Hill, Inc., New York, 1995, pp. 3–108.
34 C. W. Sill and H. E. Peterson, *Anal. Chem.*, 1947, **19**, 646–651.
35 G. Gran., *Analyst*, 1952, **77**, 661.
36 P. Di Bernardo, A. Cassol, G. Tomat, A. Bismondo and L. Magon, *J. Chem. Soc., Dalton Trans.*, 1983, 733–735.
37 P. Gans, A. Sabatini and A. Vacca, *J. Chem. Soc., Dalton Trans.*, 1985, 1195–1200.
38 I. Grenthe and H. Ots, *Acta Chem. Scand.*, 1972, **26**, 1217.
39 O. Sohnel and P. Novotny, *Densities of Aqueous Solutions of Inorganic Substances*, Elsevier, New York, 1985.
40 R. Smith, P. Zanonato and G. R. Choppin, *J. Chem. Thermodyn.*, 1992, **24**, 99–106.
41 R. Arnek, *Ark. Kemi*, 1970, **32**, 81.
42 B. J. E. Penner-Hahn, *Coord. Chem. Rev.*, 1999, **190–192**, 1101.
43 (*a*) G. G. Li, F. Bridges and C. W. Booth, *Phys. Rev. B*, 1995, **52**, 6332; (*b*) F. Bridges, C. W. Booth and G. G. Li, *Physica B*, 1995, **208–209**, 12.
44 S. I. Zabinsky, J. J. Rehr, A. Ankudinov, R. C. Albers and M. J. Eller, *Phys. Rev. B.*, 1995, **52**, 2995.